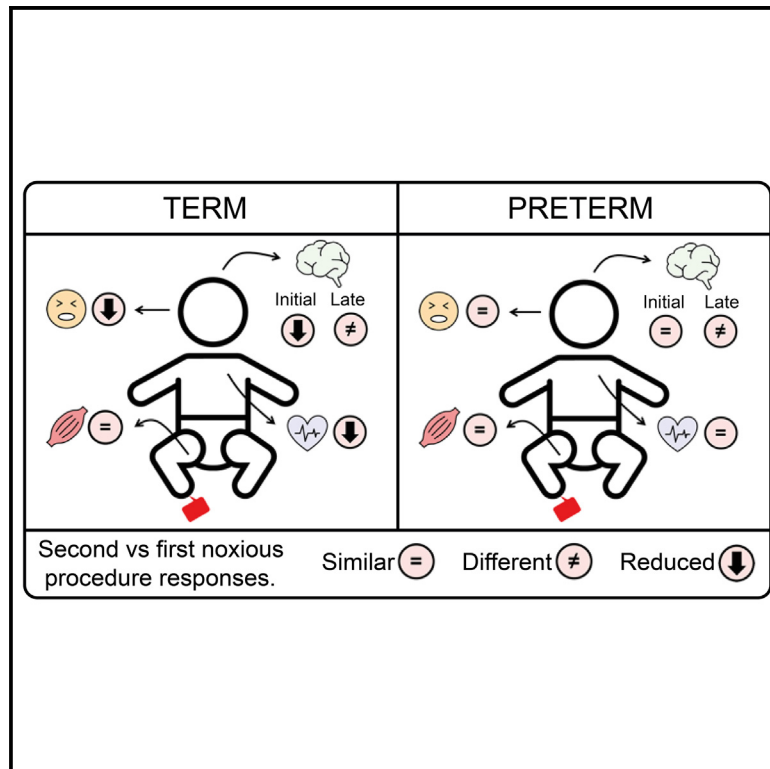


A developmental shift in habituation to pain in human neonates

Graphical abstract



Authors

Mohammed Rupawala, Oana Bucsea, Maria Pureza Laudiano-Dray, ..., Sofia Olhede, Laura Jones, Lorenzo Fabrizi

Correspondence

I.fabrizi@ucl.ac.uk

In brief

Habituation to recurrent non-threatening or unavoidable noxious stimuli is an important feature of pain adaption. Rupawala et al. provide evidence that infants at term age can adapt to repeated painful stimuli, but habituation mechanisms mature over the equivalent of the last trimester of gestation and are not fully functional in preterm neonates.

Highlights

- Term but not preterm neonates habituate to repeated unavoidable painful stimuli
- Habituation occurs in behavioral, autonomic, and early cortical responses
- Higher-level pain processing is affected by stimulus repetition in both age groups

Article

A developmental shift in habituation to pain in human neonates

Mohammed Rupawala,¹ Oana Bucsea,² Maria Pureza Laudiano-Dray,¹ Kimberley Whitehead,¹ Judith Meek,³ Maria Fitzgerald,¹ Sofia Olhede,^{4,5} Laura Jones,^{1,6} and Lorenzo Fabrizi^{1,6,7,8,9,*}

¹Department of Neuroscience, Physiology and Pharmacology, University College London, London WC1E 6BT, UK

²Faculty of Health, Department of Psychology, York University, Toronto, ON M3J 1P3, Canada

³Elizabeth Garrett Anderson Obstetric Wing, University College London Hospitals, London WC1E 6DB, UK

⁴Department of Statistical Science, University College London, London WC1E 6BT, UK

⁵Institute of Mathematics, École Polytechnique Fédérale de Lausanne, Lausanne 1015, Switzerland

⁶Senior author

⁷Twitter: @LFabriziUCL

⁸Twitter: @uclnpp

⁹Lead contact

*Correspondence: l.fabrizi@ucl.ac.uk

<https://doi.org/10.1016/j.cub.2023.02.071>

SUMMARY

Habituation to recurrent non-threatening or unavoidable noxious stimuli is an important aspect of adaptation to pain. Neonates, especially if preterm, are exposed to repeated noxious procedures during their clinical care. They can mount strong behavioral, autonomic, spinal, and cortical responses to a single noxious stimulus; however, it is not known whether the developing nervous system can adapt to the recurrence of these inputs. Here, we used electroencephalography to investigate changes in cortical microstates (representing the complex sequential processing of noxious inputs) following two consecutive clinically required heel lances in term and preterm infants. We show that stimulus repetition dampens the engagement of initial microstates and associated behavioral and autonomic responses in term infants, while preterm infants do not show signs of habituation. Nevertheless, both groups engage different longer-latency cortical microstates to each lance, which is likely to reflect changes in higher-level stimulus processing with repeated stimulation. These data suggest that while both age groups are capable of encoding contextual differences in pain, the preterm brain does not regulate the initial cortical, behavioral, and autonomic responses to repeated noxious stimuli. Habituation mechanisms to pain are already in place at term age but mature over the equivalent of the last trimester of gestation and are not fully functional in preterm neonates.

INTRODUCTION

Habituation, described as a decrease in the response to repeated stimuli, is the simplest manifestation of behavioral plasticity and is considered a basic form of memory and learning.¹ Pain is a multifaceted experience requiring extensive cortical processing that ultimately results in the appropriate behavioral and physiological responses ensuring physical integrity and survival. Pain habituation is therefore an important physiological and psychological form of adaptation to recurrent or sustained noxious stimuli and is likely to preserve physical, emotional, and cognitive resources in favor of more pressing goals when the threat is unavoidable or not life-threatening.²

Cortical activity habituates to consecutive sensory stimuli with, for example, same duration or position.³ This occurs at multiple spatial (e.g., in the individual neuronal and global cortical responses) and temporal (e.g., can last from milliseconds to days) scales.³ In the healthy adult brain, pain habituation is associated with modulation of parallel and sequential pathways⁴ including decreased activity in areas related to pain sensation—such as the thalamus, insula, and primary (SI) and

secondary (SII) somatosensory cortices—and increased activity in areas involved in descending pain modulation, such as the anterior cingulate cortex (ACC).⁵ These areas encode the sensory-discriminative, affective-motivational, and cognitive-evaluative components of the pain experience and initiate the relevant top-down signal processes that execute physical behaviors to avoid pain chronicity and resolve physical injury. These cortical processes also engage descending opioidergic mechanisms in the periaqueductal gray (PAG) projecting to the rostral ventromedial medulla (RVM), resulting in the modulation of spinal reflex response,⁶ heart rate changes,⁷ and skin conductance response.⁶

Since the nociceptive system⁸ and the nociceptive brain in particular⁹ are rapidly changing over the last trimester of human development, the mechanisms underlying habituation to a noxious stimulus are likely to mature over this period. Here, we hypothesize that the ability of the brain to adapt to recurrent noxious stimuli, and to drive appropriate behavioral and physiological responses that balance threat avoidance and energy wastage, also matures over the equivalent of the last trimester of gestation.

Table 1. Infant demographics

| | Preterm (<37 weeks PMA at study) | Term (≥ 37 weeks PMA at study) |
|---|--|--|
| Number of infants | 10 | 10 |
| GA at birth (weeks ⁺ days) | 31 ⁺⁶⁶ (24 ⁺²² –34 ⁺⁵) | 38 ⁺⁰ (31 ⁺⁶⁶ –41 ⁺⁴) |
| PNA (complete days) | 14 (5–65) | 10 (1–48) |
| PMA at study (weeks ⁺ days) | 34 ⁺⁰ (32 ⁺⁶⁶ –36 ⁺⁴) | 39 ⁺⁴⁴ (37 ⁺⁴⁴ –44 ⁺²) |
| Number of female | 5 (50%) | 4 (40%) |
| Birth weight (g) | 1,461 (708–2,240) | 3,406 (1,396–4,070) |
| Number of cesarean deliveries | 7 (70%) | 5 (50%) |
| Number of stimulation on right foot | 2 (20%) | 6 (60%) |

Note: gestational age (GA) is the number of weeks (and additional days) elapsed from the first day of the mother's last menstrual cycle to the day of delivery. Post-natal age (PNA) is the number of days elapsed since birth. Post-menstrual age (PMA) is the sum of these two ages. Values represent median and range. See also [Figure S4](#).

Testing this hypothesis requires the study of cortical network engagement and switching on a sub-second timescale. This can be achieved by performing microstate analysis on multi-channel electroencephalography (EEG) recordings to characterize the pattern of time-varying cortical potentials measured across the scalp, following a noxious stimulus.¹⁰ EEG microstate analysis reduces the complete set of spatial EEG patterns, provided as input data, to a finite, representative set of topographic maps that highlights semi-simultaneity of activity of large-scale brain networks,^{10,11} and it can provide a measurement of sequential and parallel cortical network engagement following noxious stimulation.^{12,13}

Hospitalized neonates, including those who are sick and/or born prematurely, are exposed to several noxious procedures every day as part of their clinical care.^{14–16} Heel lancing is the most common blood-sampling test in the neonatal unit and occasionally has to be repeated in quick succession to collect the required amount of blood.¹⁷ Each single lance can elicit strong behavioral, autonomic, spinal, and cortical responses in neonates, even if preterm;^{18–23} however, whether these responses decrease upon stimulus repetition is not known. Here, we present cortical, autonomic, behavioral, and reflex responses from term and preterm neonates that required two consecutive and identical clinical heel lances, and we demonstrate distinct developmental changes in the adaptation to these repeated unavoidable noxious stimuli.

RESULTS

Twenty human infants ([Table 1](#)) underwent two blood tests (heel lances) in brief succession (3–18 min separation, as clinically required) in the same heel skin area ([Figure 1](#)). This included 10 preterm (median 34 completed post-menstrual weeks, range 32–36 weeks), and 10 term equivalent (3 preterm-born and 7 term-born neonates studied at term age, median 39 completed post-menstrual weeks, range 37–44 weeks) neonates. The two

groups were significantly different in their post-menstrual age (preterm median [range]: 34.00 [32.86–36.57] weeks, term median [range]: 39.57 [37.57–44.29] weeks; Mann-Whitney U test: $z = -3.75$, $p < 0.001$) but did not differ in post-natal age (preterm median [range]: 14 [5–65] days, term median [range]: 10 [1–48] days; Mann-Whitney U test: $z = 1.44$, $p = 0.15$) nor in interstimulus interval (preterm mean [SD]: 8.91 [3.82] min, term mean [SD]: 7.11 [2.46] min; independent sample t test: $t(18) = 1.25$, $p = 0.23$, 95% CI = -1.22 to 4.82). Moreover, there was no significant change in sleep-state distribution across infants between first and second lance ([Figure S4](#), [STAR Methods](#)), and all infants (except one) stayed in the same position (cot, skin-to-skin, or held) for both lances (i.e., sleep and position were not covariates across repeated lances).

Cortical, behavioral, autonomic, and reflex responses to each lance were recorded simultaneously as follows: (1) cortical activity using scalp EEG, (2) facial expressions using video recording, (3) heart rate using electrocardiography (ECG), and (4) flexion withdrawal reflex of the stimulated limb using biceps femoris electromyography (EMG) ([Figure 1](#)).

Heel lancing engages a distinct sequence of cortical microstates in term and preterm infants

EEG responses to a heel lance were different between term and preterm infants across the scalp ([Figure 2A](#)) and at the vertex (Cz) ([Figures 2C](#), top panel; [Figure S2](#)). This was statistically confirmed by the engagement of different microstates, following stimulation ([Figures S1](#) and [S2](#)). Topographic consistency²⁷ across first (second) lance was statistically significant ($p \leq 0.05$) for 44 (22)% and 63 (61)% of the post-lance period for term and preterm infants, respectively ([Figure S1A](#)). These consistent periods were clustered into a set of nine microstates ([Figure 2B](#)), as this offered the best trade-off between data reduction and data fitting ([Figure S1B](#)).²⁸ Microstates were then assigned to a time point if the global field power (GFP) they explained was significantly higher than that explained by a random topographic basis obtained from the baseline ($p \leq 0.05$, [Figure S1C](#)). At least one microstate was assigned to 55 (55)% and 83 (94)% of the post-lance period following first (second) lance in term and preterm neonates, respectively, and overall microstate fitting explained 88% of the GFP where there was topographic consistency.

Term and preterm responses to the first lance consisted of two different sequences of 5 microstates: MS1 \rightarrow 5 \rightarrow 4 \rightarrow 7 \rightarrow 8 for term and MS1 \rightarrow 2 \rightarrow 3 \rightarrow 4 \rightarrow 6 for preterm infants ([Figure S2](#)). Only two microstates were common to the term and preterm response (MS1 and 4), while all the others were age specific. Moreover, those microstates in common had significantly lower power in term compared with preterm infants (MS1: $p = 0.001$, term 396 $\mu\text{V} \times \text{ms}$ vs. preterm 866 $\mu\text{V} \times \text{ms}$; MS4: $p < 0.001$, term 421 $\mu\text{V} \times \text{ms}$ vs. preterm 1,407 $\mu\text{V} \times \text{ms}$), started significantly earlier, and lasted significantly less (MS4 onset: $p = 0.002$, term 470 ms vs. preterm 537 ms; MS1 duration: $p = 0.007$, term 195 ms vs. preterm 479 ms; MS4 duration: $p < 0.001$, term 176 ms vs. preterm 354 ms). [Figure 2C](#) highlights both periods of dominant microstate activity, together with transitory periods where multiple states can coexist, and how these microstate activities align with the activity recorded at the vertex channel (Cz).

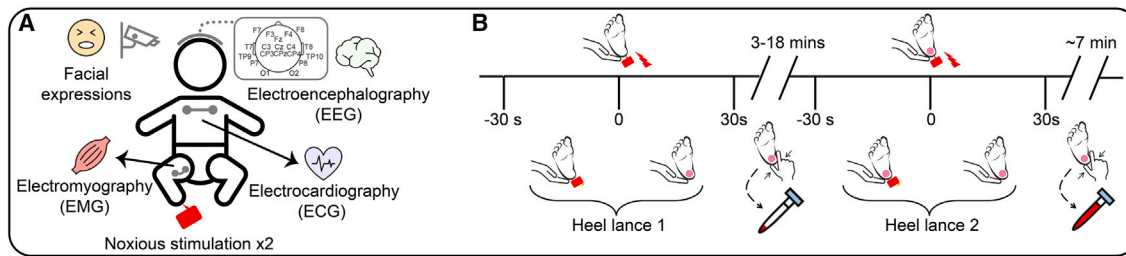


Figure 1. Study protocol

(A) Recording setup.

(B) Timeline of events. All recordings began before the first heel lance and continued for the entire duration of the study. In the 30 s preceding each lance attempt (i.e., between -30 and 0 s), the lancet was held against the heel. The lancet was released at time 0 s, and squeezing started only 30 s after to obtain a post-lance period free from other stimuli. As not enough blood was collected after the first sampling attempt, the same procedure was repeated after 3–18 min.

The initial component of the cortical response to a heel lance is suppressed following repeated stimulation in term but not preterm neonates

We first investigated the effect of heel lance repetition upon single-channel vertex (Cz) event-related potentials (ERPs) (Figure 2C, top panel). While the ERP sequence was virtually identical following first and second lance in preterm infants, it was significantly altered in the older age group. The initial component of the ERP was significantly modulated (Figure 2C, top panel). This consisted of a reduction in negative voltage up to 84 ms following the second lance compared with the first (p value range: 0.001–0.024). Changes in single-channel ERPs however may be ambiguous because they can arise from genuine changes in activity magnitude or overall voltage field configuration.²⁹ In this instance, ERP findings were confirmed by the complete obliteration of MS1 following the second lance in term neonates, while there was no change in MS1 engagement (total power and duration) in preterm infants (change in onset latency of 223 ms, $p = 0.013$). The engagement of the succeeding 2–3 microstates (MS5 and 4 in term and MS2, 3, and 4 in preterm) was independent from stimulus repetition (no difference in total power and duration, only change in MS5 onset latency of 78 ms, $p = 0.004$).

Late components of the cortical response to a heel lance are altered in both preterm and term neonates following repeated stimulation

At longer latencies, heel lance repetition in term infants led to a reverse in Cz ERP polarity between 591 and 744 ms from positive to negative (p value range: <0.001 –0.023). Microstate analysis revealed that this reverse in polarity corresponded to the engagement of a new microstate (MS6) following the second lance, which was not engaged following the first. Moreover, microstate analysis showed a complete change in the later microstates engaged from MS7 and 8 to MS9. In preterm neonates, microstate analysis also revealed a change in the later microstates engaged from MS6 to MS1 and 6, which partly corresponded to a significant reduction of the negative voltage between 1,357 and 1,445 ms following the second lance (p value range: 0.001–0.025) at Cz.

Behavioral and autonomic responses to a heel lance habituate following repeated stimulation in term but not preterm neonates

We next investigated the effect of heel lance repetition upon behavioral and autonomic responses. To do this, we compared

the changes in facial expression, heart rate, and flexion withdrawal EMG of the stimulated limb in response to first and second lance. These changes occurred in response to the same stimulus-related peripheral input that elicited the cortical response but have different timescales^{30,31} and therefore are presented on different temporal axes in Figure 3.

The first lance evoked significant changes in facial expression scores, heart rate, and biceps femoris muscle activity in both term and preterm infants ($p < 0.001$) (Figure S3). Median facial expression scores (represented as a percentage change between 0% and 100%) increased between 14.3% and 57.1% in term and between 14.3% and 71.4% in preterm infants from average baseline scores of 0% (Figures S3A and S3B); median heart rate increases were between 5.5–13.3 beats per minute (BPM) from an average resting activity of 126.1 BPM in term and 6.4–9.6 BPM from an average resting activity of 157.1 BPM in preterm infants (Figures S3C and S3D); and reflex muscle activity increases were between 2.1–3.8 standard deviations of the mean baseline activity in term and 1.1–1.7 in preterm infants (Figures S3E and S3F).

The facial expression scores and heart rate were significantly modulated by noxious stimulus repetition in term but not preterm infants. In term neonates, facial expression scores (0–4 s post-stimulus, $p = 0.009$) and heart rate changes (0–10 s post-stimulus, $p = 0.016$, and 20–30 s post-stimulus, $p = 0.011$) elicited by the second lance were significantly reduced compared with the first (Figures 3A and 3C). In preterm neonates, these two responses did not change significantly with stimulus repetition (Figures 3B and 3D). Flexion withdrawal reflex changes between first and second lance were not significantly different for both term and preterm neonates (Figures 3E and 3F).

DISCUSSION

The results presented here support the hypothesis that the ability of the nervous system to adapt to recurrent noxious stimuli matures over the equivalent of the last trimester of gestation.

To study the development of nociceptive habituation, we measured changes in cortical network engagement (microstates) following repeated clinically required noxious heel lances in term and preterm infants. Controlling for stimulus site, sleep state, and post-natal age, the results show that the initial microstate (and corresponding ERP N2) was modulated by stimulus repetition in term infants only. Importantly, autonomic (heart

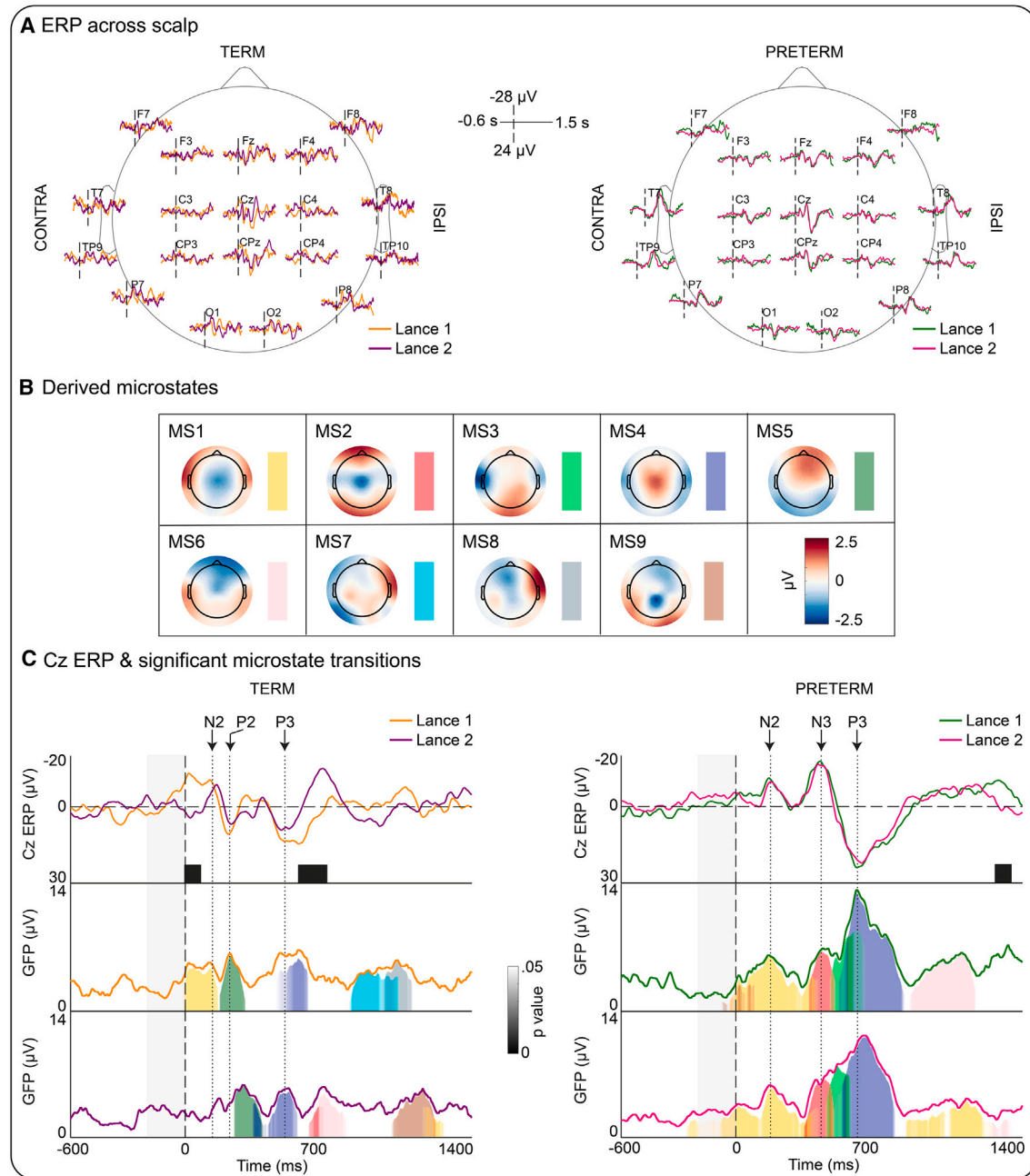


Figure 2. Initial cortical microstate engagement in response to a heel lance is modulated by stimulus repetition in term but not preterm infants, while late components of the response are altered in both age groups

Global event-related field topography (microstate) analysis of EEG responses to repeated lances in term ($n = 10$) and preterm ($n = 10$) neonates. The 0 ms stimulus marker represents the occurrence of the lance.

(A) Group average ERPs from each of the 19 channels on the infants' scalps—the left and right side of the map respectively represents electrodes contralateral and ipsilateral to the stimulus side.

(B) Microstates topographic maps. Each microstate is represented by a different color, which is used in (C).

(C) Top panel: group average ERPs at the vertex (Cz) with previously identified peaks marked.^{23–26} Black squares indicate periods of significant difference between ERP following first and second lance. Middle and bottom panels: global field power (GFP) and microstate projection on group average responses to first (middle panel) and second (bottom) lance (see STAR Methods for further details). The height of the colored blocks represents the amount of GFP explained by the corresponding microstate. We tested whether this was significantly above chance with non-parametric testing (see STAR Methods for further details). The color transparency for each microstate's projection represents the p value of this test and is summarized by the gray-scale color bar. See also Figures S1 and S2.

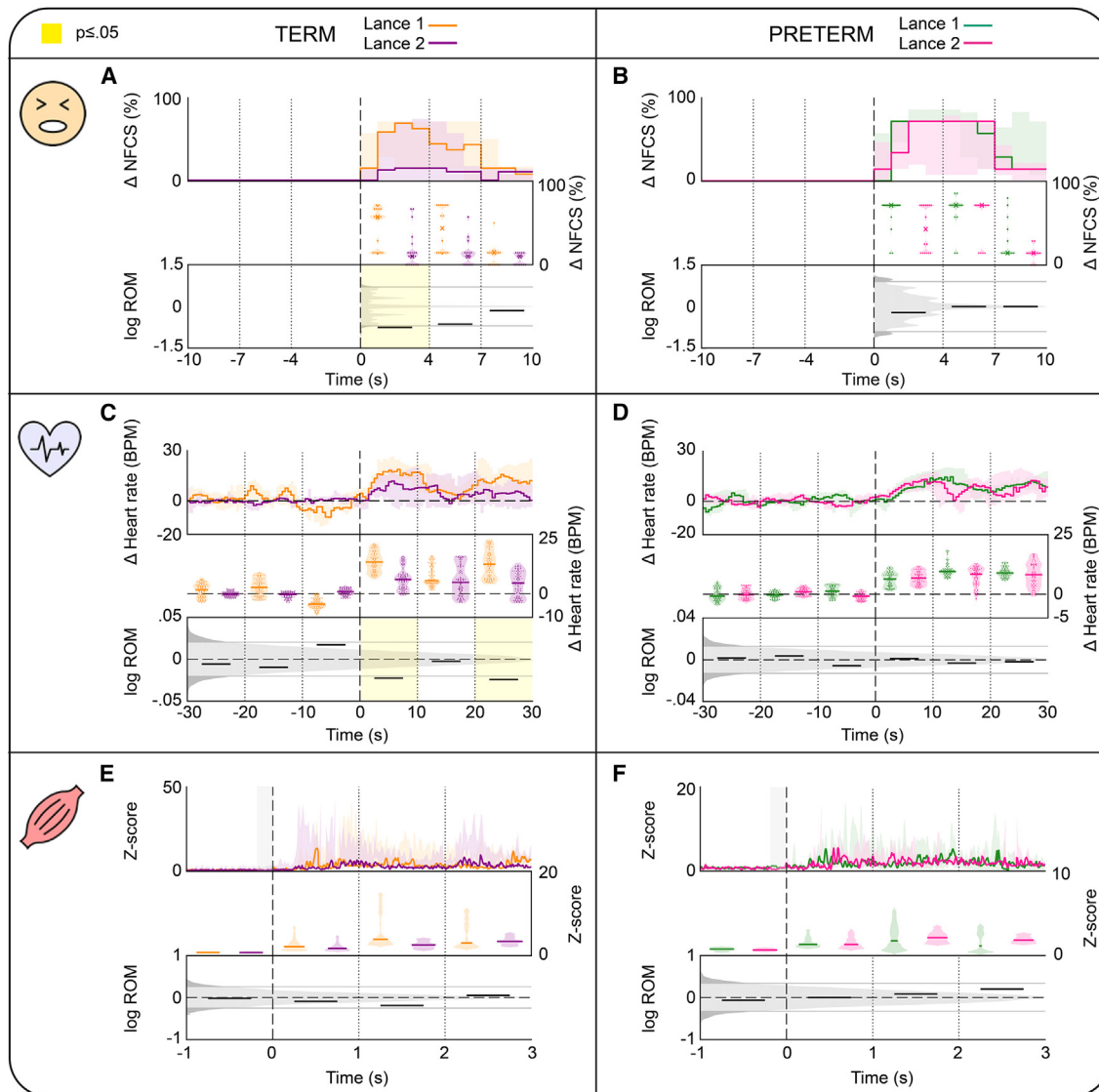


Figure 3. Noxious-evoked behavioral and autonomic responses are significantly modulated by stimulus repetition in term but not preterm infants

Comparison between responses in term (left) and preterm (right) infants to first and second lance. The 0 ms stimulus marker represents the occurrence of the lance.

(A and B) Differences in facial expression scores (recorded using video and evaluated using Neonatal Facial Coding System [NFCS]) (term $n = 10$, preterm $n = 9$) (term: 0–4 s post-stimulus, $p = 0.009$).

(C and D) Differences in heart rate (derived from ECG) (term $n = 10$, preterm $n = 9$) (term: 0–10 s post-stimulus, $p = 0.016$; 20–30 s post-stimulus, $p = 0.011$).

(E and F) Differences in the flexion withdrawal reflex of the biceps femoris (EMG) (term $n = 5$, preterm $n = 4$). Top panel: traces represent the median response across subjects. Shaded areas represent the interquartile range at each time point. Middle panel: solid lines represent the median response across subjects/temporal window for each lance. Violin plots represent data distribution within the interquartile range. Bottom panel: solid black lines represent the log ratio of the median (ROM) responses to the two lances within each temporal window. These ratios were tested against a non-parametric distribution of surrogate ratios (shaded gray) (see STAR Methods for further details on surrogate data generation). Dark gray regions represent values below the 2.5th and above the 97.5th percentiles (solid gray lines). The null hypothesis was rejected if the ratios calculated from the original data were outside these percentiles. Yellow areas represent time windows with significant differences between first and second lance. See also Figure S3.

rate) and behavioral (facial expression) responses also habituated in term but not preterm infants. Nevertheless, both age groups showed changes in the late part of their cortical responses, beyond simple activity modulation, revealing potential differences in higher cortical processing with repeated identical noxious stimulation. These results suggest that the modulatory

mechanisms responsible for habituation and altered cortical processing to repeated noxious procedures undergo a developmental shift between preterm and term age.

Traditional single-channel vertex ERP analysis has been used extensively to explore responses to noxious stimuli in neonates.³² This analysis has led to the identification of a specific

voltage deflection (the P3 potential at Cz), which is associated with the tissue-breaking aspect of the stimulus.²³ However, considering the complexity of the pain experience and of the brain networks engaged in the processing of noxious input,⁴ this approach could be reductive and fail to capture the multifaceted temporospatial dynamics of nociceptive cortical processing. Unlike entire scalp topographies, single-channel analysis is (1) noisier, as it relies on a single spatial sample when multiple channel recordings are available; (2) reference dependent; and (3) can present erroneous magnitude differences when there are latency shifts or changes in voltage field distribution.³³ On the other hand, topographic information as used here has direct neurophysiologic interpretability, in that pattern differences in time and space (microstates) reflect changes in the configuration of active cerebral sources.³³ Previously described N2-related and nociceptive complex (N3-P3)-related topographies^{26,34–36} were identified here as MS1(N2) and MS4 (P3) in both term and preterm neonates and as MS2 (N3) in preterm neonates only. However, microstate analysis identified another six microstates, which would have otherwise been missed with traditional ERP analysis as they were not associated with peaks at the scalp vertex (Cz). Considering EEG microstates as a continuous phenomenon³⁷ has also allowed us to identify periods of dominant single microstate activation, together with others of overlapping multi-microstates coexistence and smooth transitory intervals between dominant microstates. The median duration for the microstates obtained here was approximately 200 ms. Typically, canonical microstates in adults have a duration of between 60 and 150 ms;¹⁰ however, other studies in neonates report longer durations of 150–300 ms.^{12,38,39} It is therefore possible that microstates last longer in neonates, compared with adults, perhaps due to a simpler network that only allows for relatively slower switching between processes.

While the functional significance of ERP and microstates have not been conclusively defined, increases in latency and topographic complexity are thought to reflect increasing integration of information and higher-order function in adults⁴⁰ as well as neonates.⁴¹ Initial microstates engaged in response to a heel lance are related to nociceptive facial expression in preterm and term neonates.¹² In animal models, autonomic responses and reflexive escape behaviors are mediated by the activation of the spino-parabrachial pathway (in the dorsolateral pons).^{42–45} The initial microstate and behavioral, and autonomic responses could therefore be linked to the activation of this pathway, which conveys information to the ACC and limbic regions.^{46–49} Indeed, neonatal facial actions are driven by motor neurons in the pons of the brainstem and are considered reflexive behaviors to bring about caregiver proximity.⁹ Therefore, the reduction in the first EEG microstate (and corresponding ERP N2) and behavioral and autonomic responses to stimulus repetition may reflect fast-acting modulatory mechanisms of pathways that are related to these reflexive survival behaviors.

The mechanisms underlying these diminished responses are not known but may be a consequence of neuronal fatigue whereby neurons initially responsive show a reduction in firing rate to repeated presentations of the same stimulus (passive habituation).³ Alternatively, the reduction in activity may be a consequence of a sharpening model whereby the activity of networks encoding features irrelevant to the identification of a

stimulus is suppressed (active suppression).^{50,51} Top-down models, on the other hand, propose that cortical activity changes arise from the integration of sensory input with predictions about the expected stimulus, based on a continuously updated internal model of the world.⁵² Only differences between the expected and received input would therefore lead to a prediction error reflected in the activation of pain-related brain areas.^{53,54} In this framework, habituation would represent the ability of the brain to compare and successfully predict the arrival of successive stimuli.⁵⁵ In adults, stimulus expectancy is reflected in ERP amplitude changes.⁵⁶ Specifically, the earliest ERPs are modulated by the prediction of the incoming stimulus,^{57,58} whereas later responses correlate with the prediction error.⁵⁹ In this model, cortical predictions in neonates undergoing repeated blood tests may develop through associative learning processes that are already possible by term age (classical conditioning),⁶⁰ with holding and preparation of the heel before the lance functioning as the conditioning stimulus. Generally, animals act to terminate or avoid pain by responding appropriately to noxious-related cues,⁶¹ which in the absence of other conflicting goals (e.g., need for feeding) would result in the amplification of nociceptive transmission to guide such behaviors. However, this is only useful when avoidance is possible, which is not the case for human neonates undergoing a heel lance. In this case, it is likely that the cue signaling imminent pain drives the engagement of modulatory mechanisms that reduce the nociceptive input. The shift from non-habituation in preterm to habituation in term infants could therefore be related to maturational changes in these processes, a change in the mechanisms through which they are engaged, or both.

Top-down control of pain involves multiple forebrain regions connecting with the PAG region and RVM in the brainstem, which regulates nociceptive transmission at the dorsal horn level.⁶² In term neonates, stronger spontaneous pre-stimulus functional connectivity across this descending pain modulatory system predicts a weaker response to a mechanical pin-prick.⁶³ However, this control network is immature in animal models at the equivalent age to human preterm neonates: the descending projections from the brainstem to the dorsal horn are anatomically present, but their inhibitory function is not fully developed.^{64–66} These maturational changes potentially explain the modulation of the responses in heart rate change, facial behaviors, and initial cortical events that was present in term but not preterm neonates. However, given these potential developmental changes in physiology, it is surprising that no significant changes were observed in their spinally mediated withdrawal reflex. This may be attributed to the low number of trials with EMG recordings from which the observed effects were estimated.

Unlike the initial microstate, long-latency microstates were unique, following each lance procedure in both preterm and term neonates. These late microstates could represent the activation of the anti-nociceptive⁵ or cognitive-evaluative⁶⁷ networks that modulate subsequent incoming noxious-related signals and/or assess contextual/environmental factors⁶⁸ or could encode the prediction errors in the predictive coding framework.⁵⁹ These networks involve high-level brain regions (e.g., ACC and prefrontal cortex) and together are involved in the prediction or avoidance of noxious stimuli.^{69,70} Both preterm and term neonates demonstrate the potential for high-level

processing of contextual differences pertaining to each noxious event. However, preterm neonates seem unable to use this information to regulate brainstem and thalamocortical control over reflexive behavior, autonomic responses, and initial cortical activation.

This is the first study to demonstrate the neural and physiological implications of closely repeated noxious clinical procedures in human neonates. Unlike term infants, preterm infants fail to habituate to repeated pain yet engage neuronal activity patterns suggestive of distinct high-level cortical processing of each noxious event. Given that the preterm architecture is generally geared toward activity-dependent sensory development with low inhibition and high facilitation of inputs, noxious clinical procedures may possibly introduce undesirable and untimely changes, negatively impacting the neonate's developmental trajectory. Indeed, these injury-induced changes to the developing brain are known to result in maladaptive cortical-pain processing and pain-related behaviors, associated with negative outcomes later in life, or in long-lasting disabilities.⁷¹ Moreover, preterm-born neonates at term equivalent age, who spent an average of 87 days in neonatal care, have similar but stronger cortical responses as term-born neonates to a noxious stimulus.²⁴ The same could be true for the three preterm-born neonates studied at term in this study; however, most importantly, the median time spent in neonatal care was less than 2 weeks and not significantly different between the preterm and term group. In future studies it will be important to assess the effect of extrauterine experience on the adaptation processes described in this study.

In conclusion, this work increases our neurophysiological understanding of infant brain responses and behaviors to repeated noxious stimulation. The data suggest that the preterm brain is capable of encoding high-level contextual differences in pain but cannot adapt to repeated unavoidable noxious stimuli potentially because of developmental inability/delay in their learning ability or in engaging the necessary control systems. The failure of the preterm brain to adapt to repeated noxious stimulation emphasizes the vulnerability of preterm infants to repeated painful procedures during their stay in a neonatal intensive care unit.

STAR★METHODS

Detailed methods are provided in the online version of this paper and include the following:

- **KEY RESOURCES TABLE**
- **RESOURCE AVAILABILITY**
 - Lead contact
 - Materials availability
 - Data and code availability
- **EXPERIMENTAL MODEL AND SUBJECT DETAILS**
- **METHOD DETAILS**
 - Repeated noxious stimuli
 - Data collection
 - EEG recording and preprocessing
 - EMG recording and preprocessing
 - ECG recording and preprocessing
 - Facial expression recording and preprocessing
 - EEG microstate analysis
- **QUANTIFICATION AND STATISTICAL ANALYSIS**

- Cortical response quantification and statistical comparison across ages and stimulus repetition
- Behavioural, spinal reflex, and autonomic response to a noxious stimulus quantification and analysis
- Behavioural, spinal reflex, and autonomic response statistical comparison across stimulus repetition
- Surrogate data generation

SUPPLEMENTAL INFORMATION

Supplemental information can be found online at <https://doi.org/10.1016/j.cub.2023.02.071>.

ACKNOWLEDGMENTS

This work was funded by the Medical Research Council UK (MR/S003207/1) and the European Research Council (CoG 2015-682172NETS) within the Seventh European Union Framework Program. O.B. was supported by the Canadian Institutes of Health Research (FBD-170829). The research was performed at the University College London Hospitals (UCLH) Maternity and Neonatal Units. The authors thank the families of the infants that participated in this research. The authors also thank Stephanie Koch for discussions of the results. For the purpose of open access, the author has applied a Creative Commons Attribution (CC BY) license to any Author Accepted Manuscript version arising.

AUTHOR CONTRIBUTIONS

Conceptualization of study, L.J., L.F., and M.F.; data collection and preparation, L.J., M.P.L.-D., and K.W.; clinical supervision, J.M.; data analysis, M.R., L.J., O.B., and S.O.; data interpretation, M.R., L.J., and L.F.; manuscript preparation, M.R., L.J., and L.F. All authors discussed the results and commented on the manuscript.

DECLARATION OF INTERESTS

The authors declare no competing interests.

Received: April 29, 2022
Revised: November 22, 2022
Accepted: February 23, 2023
Published: March 16, 2023

REFERENCES

1. Groves, P.M., and Thompson, R.F. (1970). Habituation: a dual-process theory. *Psychol. Rev.* 77, 419–450. <https://doi.org/10.1037/h0029810>.
2. De Paepe, A.L., Williams, A.C.C., and Crombez, G. (2019). Habituation to pain: a motivational-ethological perspective. *Pain* 160, 1693–1697. <https://doi.org/10.1097/j.pain.0000000000001533>.
3. Grill-Spector, K., Henson, R., and Martin, A. (2006). Repetition and the brain: neural models of stimulus-specific effects. *Trends Cogn. Sci.* 10, 14–23. <https://doi.org/10.1016/j.tics.2005.11.006>.
4. Kucyi, A., and Davis, K.D. (2015). The dynamic pain connectome. *Trends Neurosci.* 38, 86–95. <https://doi.org/10.1016/j.tins.2014.11.006>.
5. Bingel, U., Schoell, E., Herken, W., Büchel, C., and May, A. (2007). Habituation to painful stimulation involves the anti nociceptive system. *Pain* 131, 21–30. <https://doi.org/10.1016/j.pain.2006.12.005>.
6. Bromm, B., and Scharein, E. (1982). Response plasticity of pain evoked reactions in man. *Physiol. Behav.* 28, 109–116. [https://doi.org/10.1016/0031-9384\(82\)90111-1](https://doi.org/10.1016/0031-9384(82)90111-1).
7. Colloca, L., Benedetti, F., and Pollo, A. (2006). Repeatability of autonomic responses to pain anticipation and pain stimulation. *Eur. J. Pain* 10, 659–665. <https://doi.org/10.1016/j.ejpain.2005.10.009>.

8. Fitzgerald, M., and Walker, S.M. (2009). Infant pain management: a developmental neurobiological approach. *Nat. Clin. Pract. Neurol.* 5, 35–50. <https://doi.org/10.1038/ncpneuro0984>.
9. Verriotis, M., Chang, P., Fitzgerald, M., and Fabrizi, L. (2016). The development of the nociceptive brain. *Neuroscience* 338, 207–219. <https://doi.org/10.1016/j.neuroscience.2016.07.026>.
10. Michel, C.M., and Koenig, T. (2018). EEG microstates as a tool for studying the temporal dynamics of whole-brain neuronal networks: a review. *NeuroImage* 180, 577–593. <https://doi.org/10.1016/j.neuroimage.2017.11.062>.
11. von Wegner, F., Knaut, P., and Laufs, H. (2018). EEG microstates sequences from different clustering algorithms are information-theoretically invariant. *Front. Comput. Neurosci.* 12, 70. <https://doi.org/10.3389/fncom.2018.00070>.
12. Bucsea, O., Rupawala, M., Shiff, I., Wang, X., Meek, J., Fitzgerald, M., Fabrizi, L., Riddell, R.P., and Jones, L. (2022). Clinical thresholds in pain-related facial activity linked to differences in cortical network activation in neonates. *Pain*. <https://doi.org/10.1097/j.pain.0000000000002798>.
13. May, E.S., Gil Ávila, C., Ta Dinh, S., Heitmann, H., Hohn, V.D., Nickel, M.M., Tiemann, L., Tölle, T.R., and Ploner, M. (2021). Dynamics of brain function in patients with chronic pain assessed by microstate analysis of resting-state electroencephalography. *Pain* 162, 2894–2908. <https://doi.org/10.1097/j.pain.0000000000002281>.
14. Cruz, M.D., Fernandes, A.M., and Oliveira, C.R. (2016). Epidemiology of painful procedures performed in neonates: a systematic review of observational studies. *Eur. J. Pain* 20, 489–498. <https://doi.org/10.1002/ejp.757>.
15. Kassab, M., Alhassan, A.A., Alzoubi, K.H., and Khader, Y.S. (2019). Number and frequency of routinely applied painful procedures in university neonatal intensive care unit. *Clin. Nurs. Res.* 28, 488–501. <https://doi.org/10.1177/1054773817744324>.
16. Laudiano-Dray, M.P., Pillai Riddell, R., Jones, L., Iyer, R., Whitehead, K., Fitzgerald, M., Fabrizi, L., and Meek, J. (2020). Quantification of neonatal procedural pain severity: a platform for estimating total pain burden in individual infants. *Pain* 161, 1270–1277. <https://doi.org/10.1097/j.pain.0000000000001814>.
17. Shah, V.S., and Ohlsson, A. (2011). Venepuncture versus heel lance for blood sampling in term neonates. *Cochrane Database Syst. Rev.* 2011, CD001452. <https://doi.org/10.1002/14651858.CD001452.pub4>.
18. Cornelissen, L., Fabrizi, L., Patten, D., Worley, A., Meek, J., Boyd, S., Slater, R., and Fitzgerald, M. (2013). Postnatal temporal, spatial and modality tuning of nociceptive cutaneous flexion reflexes in human infants. *PLoS One* 8, e76470. <https://doi.org/10.1371/journal.pone.0076470>.
19. Johnston, C.C., Stevens, B., Pinelli, J., Gibbins, S., Filion, F., Jack, A., Steele, S., Boyer, K., and Veilleux, A. (2003). Kangaroo care is effective in diminishing pain response in preterm neonates. *Arch. Pediatr. Adolesc. Med.* 157, 1084–1088. <https://doi.org/10.1001/archpedi.157.11.1084>.
20. Jones, L., Fabrizi, L., Laudiano-Dray, M., Whitehead, K., Meek, J., Verriotis, M., and Fitzgerald, M. (2017). Nociceptive cortical activity is dissociated from nociceptive behavior in new born human infants under stress. *Curr. Biol.* 27, 3846.e3–3851.e3. <https://doi.org/10.1016/j.cub.2017.10.063>.
21. Waxman, J.A., Pillai Riddell, R.R., Tablon, P., Schmidt, L.A., and Pinhasov, A. (2016). Development of cardio vascular indices of acute pain responding in infants: a systematic review. *Pain Res. Manag.* 2016, 8458696. <https://doi.org/10.1155/2016/8458696>.
22. Slater, R., Cornelissen, L., Fabrizi, L., Patten, D., Yoxen, J., Worley, A., Boyd, S., Meek, J., and Fitzgerald, M. (2010). Oral sucrose as an analgesic drug for procedural pain in newborn infants: a randomised controlled trial. *Lancet* 376, 1225–1232. [https://doi.org/10.1016/S0140-6736\(10\)61303-7](https://doi.org/10.1016/S0140-6736(10)61303-7).
23. Slater, R., Worley, A., Fabrizi, L., Roberts, S., Meek, J., Boyd, S., and Fitzgerald, M. (2010). Evoked potentials generated by noxious stimulation in the human infant brain. *Eur. J. Pain* 14, 321–326. <https://doi.org/10.1016/j.ejpain.2009.05.005>.
24. Slater, R., Fabrizi, L., Worley, A., Meek, J., Boyd, S., and Fitzgerald, M. (2010). Premature infants display increased noxious-evoked neuronal activity in the brain compared to healthy age-matched term-born infants. *NeuroImage* 52, 583–589. <https://doi.org/10.1016/j.neuroimage.2010.04.253>.
25. Fabrizi, L., Slater, R., Worley, A., Meek, J., Boyd, S., Olhede, S., and Fitzgerald, M. (2011). A shift in sensory processing that enables the developing human brain to discriminate touch from pain. *Curr. Biol.* 21, 1552–1558. <https://doi.org/10.1016/j.cub.2011.08.010>.
26. Verriotis, M., Fabrizi, L., Lee, A., Cooper, R.J., Fitzgerald, M., and Meek, J. (2016). Mapping cortical responses to somato sensory stimuli in human infants with simultaneous near-infrared spectroscopy and event-related potential recording. *eNeuro* 3, ENEURO.0026-16.2016. <https://doi.org/10.1523/ENEURO.0026-16.2016>.
27. Koenig, T., and Melie-García, L. (2010). A method to determine the presence of averaged event-related fields using randomization tests. *Brain Topogr.* 23, 233–242. <https://doi.org/10.1007/s10548-010-0142-1>.
28. Habermann, M., Weusmann, D., Stein, M., and Koenig, T. (2018). A Student's guide to randomization statistics for multi channel event-related potentials using Ragu. *Front. Neurosci.* 12, 355. <https://doi.org/10.3389/fnins.2018.00355>.
29. Pourtois, G., Delplanque, S., Michel, C., and Vuilleumier, P. (2008). Beyond conventional event-related brain potential (ERP): exploring the time-course of visual emotion processing using topographic and principal component analyses. *Brain Topogr.* 20, 265–277. <https://doi.org/10.1007/s10548-008-0053-6>.
30. Worley, A., Fabrizi, L., Boyd, S., and Slater, R. (2012). Multi-modal pain measurements in infants. *J. Neurosci. Methods* 205, 252–257. <https://doi.org/10.1016/j.jneumeth.2012.01.009>.
31. Roué, J.M., Rioualen, S., Gendras, J., Misery, L., Gouillou, M., and Sizun, J. (2018). Multi-modal pain assessment: are near-infrared spectroscopy, skin conductance, salivary cortisol, physiologic parameters, and neonatal facial coding system interrelated during venepuncture in healthy, term neonates? *J. Pain Res.* 11, 2257–2267. <https://doi.org/10.2147/JPR.S165810>.
32. Shiroshita, Y., Kirimoto, H., Ozawa, M., Watanabe, T., Uematsu, H., Yunoki, K., and Sobue, I. (2021). Can event-related potentials evoked by heel lance assess pain processing in neonates? A systematic review. *Children (Basel)* 8, 58. <https://doi.org/10.3390/children8020058>.
33. Michel, C.M., and Murray, M.M. (2012). Towards the utilization of EEG as a brain imaging tool. *NeuroImage* 61, 371–385. <https://doi.org/10.1016/j.neuroimage.2011.12.039>.
34. Jones, L., Laudiano-Dray, M.P., Whitehead, K., Verriotis, M., Meek, J., Fitzgerald, M., and Fabrizi, L. (2018). EEG, behavioural and physiological recordings following a painful procedure in human neonates. *Sci. Data* 5, 180248. <https://doi.org/10.1038/sdata.2018.248>.
35. van der Vaart, M., Hartley, C., Baxter, L., Mellado, G.S., Andritsou, F., Cobo, M.M., Fry, R.E., Adams, E., Fitzgibbon, S., and Slater, R. (2022). Premature infants display discriminable behavioral, physiological, and brain responses to noxious and nonnoxious stimuli. *Cereb. Cortex* 32, 3799–3815. <https://doi.org/10.1093/cercor/bhab449>.
36. Hartley, C., Duff, E.P., Green, G., Mellado, G.S., Worley, A., Rogers, R., and Slater, R. (2017). Nociceptive brain activity as a measure of analgesic efficacy in infants. *Sci. Transl. Med.* 9, eaah6122. <https://doi.org/10.1126/scitranslmed.aah6122>.
37. Mishra, A., Englitz, B., and Cohen, M.X. (2020). EEG microstates as a continuous phenomenon. *NeuroImage* 208, 116454. <https://doi.org/10.1016/j.neuroimage.2019.116454>.
38. Khazaei, M., Raeisi, K., Croce, P., Tamburro, G., Tokariev, A., Vanhatalo, S., Zappasodi, F., and Comani, S. (2021). Characterization of the functional dynamics in the neonatal brain during REM and NREM sleep states by means of microstate analysis. *Brain Topogr.* 34, 555–567. <https://doi.org/10.1007/s10548-021-00861-1>.
39. Jones, L., Laudiano-Dray, M.P., Whitehead, K., Meek, J., Fitzgerald, M., Fabrizi, L., and Pillai Riddell, R.P. (2021). The impact of parental contact

- upon cortical noxious-related activity in human neonates. *Eur. J. Pain* 25, 149–159. <https://doi.org/10.1002/ejp.1656>.
40. Bastuji, H., Frot, M., Perchet, C., Magnin, M., and Garcia-Larrea, L. (2016). Pain networks from the inside: spatiotemporal analysis of brain responses leading from nociception to conscious perception. *Hum. Brain Mapp.* 37, 4301–4315. <https://doi.org/10.1002/hbm.23310>.
41. Whitehead, K., Papadelis, C., Laudiano-Dray, M.P., Meek, J., and Fabrizi, L. (2019). The emergence of hierarchical somatosensory processing in late prematurity. *Cereb. Cortex* 29, 2245–2260. <https://doi.org/10.1093/cercor/bhz030>.
42. Chiang, M.C., Nguyen, E.K., Canto-Bustos, M., Papale, A.E., Oswald, A.-M.M., and Ross, S.E. (2020). Divergent neural pathways emanating from the lateral para brachial nucleus mediate distinct components of the pain response. *Neuron* 106, 927–939.e5. <https://doi.org/10.1016/j.neuron.2020.03.014>.
43. Choi, S., Hachisuka, J., Brett, M.A., Magee, A.R., Omori, Y., Iqbal, N.U., Zhang, D., DeLisle, M.M., Wolfson, R.L., Bai, L., et al. (2020). Parallel ascending spinal pathways for affective touch and pain. *Nature* 587, 258–263. <https://doi.org/10.1038/s41586-020-2860-1>.
44. Williams, A.C.de C. (2002). Facial expression of pain: an evolutionary account. *Behav. Brain Sci.* 25, 439–455. , discussion 455–488. <https://doi.org/10.1017/s0140525x02000080>.
45. Kang, S.J., Liu, S., Ye, M., Kim, D.-I., Kim, J.-H., Oh, T.G., Peng, J., Evans, R.M., Lee, K.-F., Goulding, M., and Han, S. (2020). Unified neural pathways that gate affective pain and multisensory innate threat signals to the amygdala. <https://doi.org/10.1101/2020.11.17.385104>.
46. Bushnell, M.C., Čeko, M., and Low, L.A. (2013). Cognitive and emotional control of pain and its disruption in chronic pain. *Nat. Rev. Neurosci.* 14, 502–511. <https://doi.org/10.1038/nrn3516>.
47. Rainville, P., Duncan, G.H., Price, D.D., Carrier, B., and Bushnell, M.C. (1997). Pain affect encoded in human anterior cingulate but not somatosensory cortex. *Science* 277, 968–971. <https://doi.org/10.1126/science.277.5328.968>.
48. Todd, A.J. (2010). Neuronal circuitry for pain processing in the dorsal horn. *Nat. Rev. Neurosci.* 11, 823–836. <https://doi.org/10.1038/nrn2947>.
49. Xiao, Z., Martinez, E., Kulkarni, P.M., Zhang, Q., Hou, Q., Rosenberg, D., Talay, R., Shalot, L., Zhou, H., Wang, J., et al. (2019). Cortical pain processing in the rat anterior cingulate cortex and primary somatosensory cortex. *Front. Cell. Neurosci.* 13, 165. <https://doi.org/10.3389/fncel.2019.00165>.
50. Wiggs, C.L., and Martin, A. (1998). Properties and mechanisms of perceptual priming. *Curr. Opin. Neurobiol.* 8, 227–233. [https://doi.org/10.1016/s0959-4388\(98\)80144-x](https://doi.org/10.1016/s0959-4388(98)80144-x).
51. Desimone, R. (1996). Neural mechanisms for visual memory and their role in attention. *Proc. Natl. Acad. Sci. USA* 93, 13494–13499. <https://doi.org/10.1073/pnas.93.24.13494>.
52. Friston, K., and Kiebel, S. (2009). Predictive coding under the free-energy principle. *Philos. Trans. R. Soc. Lond. B Biol. Sci.* 364, 1211–1221. <https://doi.org/10.1098/rstb.2008.0300>.
53. Geuter, S., Boll, S., Eippert, F., and Büchel, C. (2017). Functional dissociation of stimulus intensity encoding and predictive coding of pain in the insula. *eLife* 6, e24770. <https://doi.org/10.7554/eLife.24770>.
54. Wang, S., Veinot, J., Goyal, A., Khatibi, A., Lazar, S.W., and Hashmi, J.A. (2022). Distinct networks of periaqueductal gray columns in pain and threat processing. *NeuroImage* 250, 118936. <https://doi.org/10.1016/j.neuroimage.2022.118936>.
55. Seymour, B., and Mancini, F. (2020). Hierarchical models of pain: inference, information-seeking, and adaptive control. *NeuroImage* 222, 117212. <https://doi.org/10.1016/j.neuroimage.2020.117212>.
56. Hird, E.J., Jones, A.K.P., Talmi, D., and El-Deredey, W. (2018). A comparison between the neural correlates of laser and electric pain stimulation and their modulation by expectation. *J. Neurosci. Methods* 293, 117–127. <https://doi.org/10.1016/j.jneumeth.2017.09.011>.
57. Bendixen, A., SanMiguel, I., and Schröger, E. (2012). Early electrophysiological indicators for predictive processing in audition: a review. *Int. J. Psychophysiol.* 83, 120–131. <https://doi.org/10.1016/j.ijpsycho.2011.08.003>.
58. Rauss, K., Schwartz, S., and Pourtois, G. (2011). Top-down effects on early visual processing in humans: a predictive coding framework. *Neurosci. Biobehav. Rev.* 35, 1237–1253. <https://doi.org/10.1016/j.neubiorev.2010.12.011>.
59. Stefanics, G., Heinze, J., Horváth, A.A., and Stephan, K.E. (2018). Visual mismatch and predictive coding: a computational single-trial ERP study. *J. Neurosci.* 38, 4020–4030. <https://doi.org/10.1523/JNEUROSCI.3365-17.2018>.
60. Dall’Orso, S., Fifer, W.P., Balsam, P.D., Brandon, J., O’Keefe, C., Poppe, T., Vecchiato, K., Edwards, A.D., Burdet, E., and Arichi, T. (2021). Cortical processing of multimodal sensory learning in human neonates. *Cereb. Cortex* 31, 1827–1836. <https://doi.org/10.1093/cercor/bhaa340>.
61. Fields, H.L. (2018). How expectations influence pain. *Pain* 159 (Suppl 1), S3–S10. <https://doi.org/10.1097/j.pain.0000000000001272>.
62. Millan, M.J. (2002). Descending control of pain. *Prog. Neurobiol.* 66, 355–474. [https://doi.org/10.1016/s0301-0082\(02\)00009-6](https://doi.org/10.1016/s0301-0082(02)00009-6).
63. Goksan, S., Baxter, L., Moultrie, F., Duff, E., Hathway, G., Hartley, C., Tracey, I., and Slater, R. (2018). The influence of the descending pain modulatory system on infant pain-related brain activity. *eLife* 7, e37125. <https://doi.org/10.7554/eLife.37125>.
64. Hathway, G.J., Koch, S., Low, L., and Fitzgerald, M. (2009). The changing balance of brainstem–spinal cord modulation of pain processing over the first weeks of rat postnatal life. *J. Physiol.* 587, 2927–2935. <https://doi.org/10.1113/jphysiol.2008.168013>.
65. deKort, A.R., Joosten, E.A.J., Patijn, J., Tibboel, D., and van den Hoogen, N.J. (2021). The development of descending serotonergic modulation of the spinal nociceptive network: a life span perspective. *Pediatr. Res.* 91, 1361–1369. <https://doi.org/10.1038/s41390-021-01638-9>.
66. Koch, S.C., and Fitzgerald, M. (2014). The selectivity of rostroventral medulla descending control of spinal sensory inputs shifts postnatally from A fibre to C fibre evoked activity. *J. Physiol.* 592, 1535–1544. <https://doi.org/10.1113/jphysiol.2013.267518>.
67. Petrovic, P., and Ingvar, M. (2002). Imaging cognitive modulation of pain processing. *Pain* 95, 1–5. [https://doi.org/10.1016/S0304-3959\(01\)00467-5](https://doi.org/10.1016/S0304-3959(01)00467-5).
68. Tracey, I., and Mantyh, P.W. (2007). The cerebral signature for pain perception and its modulation. *Neuron* 55, 377–391. <https://doi.org/10.1016/j.neuron.2007.07.012>.
69. Coghill, R.C., Sang, C.N., Maisog, J.M., and Iadarola, M.J. (1999). Pain intensity processing within the human brain: a bilateral, distributed mechanism. *J. Neurophysiol.* 82, 1934–1943. <https://doi.org/10.1152/jn.1999.82.4.1934>.
70. Villemure, C., and Bushnell, C.M. (2002). Cognitive modulation of pain: how do attention and emotion influence pain processing? *Pain* 95, 195–199. [https://doi.org/10.1016/S0304-3959\(02\)00007-6](https://doi.org/10.1016/S0304-3959(02)00007-6).
71. Williams, M.D., and Lascelles, B.D.X. (2020). Early neonatal pain—review of clinical and experimental implications on painful conditions later in life. *Front. Pediatr.* 8, 30. <https://doi.org/10.3389/fped.2020.00030>.
72. Grunau, R.V.E., and Craig, K.D. (1987). Pain expression in neonates: facial action and cry. *Pain* 28, 395–410. [https://doi.org/10.1016/0304-3959\(87\)90073-X](https://doi.org/10.1016/0304-3959(87)90073-X).
73. Homan, R.W., Herman, J., and Purdy, P. (1987). Cerebral location of international 10–20 system electrode placement. *Electroencephalogr. Clin. Neurophysiol.* 66, 376–382. [https://doi.org/10.1016/0013-4694\(87\)90206-9](https://doi.org/10.1016/0013-4694(87)90206-9).
74. Delorme, A., and Makeig, S. (2004). EEGLAB: an open source toolbox for analysis of single-trial EEG dynamics including independent component analysis. *J. Neurosci. Methods* 134, 9–21. <https://doi.org/10.1016/j.jneumeth.2003.10.009>.

75. Leys, C., Ley, C., Klein, O., Bernard, P., and Licata, L. (2013). Detecting outliers: do not use standard deviation around the mean, use absolute deviation around the median. *J. Exp. Soc. Psychol.* *49*, 764–766. <https://doi.org/10.1016/j.jesp.2013.03.013>.
76. AholaKohut, S., and Pillai Riddell, R. (2009). Does the neonatal facial coding system differentiate between infants experiencing pain-related and non-pain-related distress? *J. Pain* *10*, 214–220. <https://doi.org/10.1016/j.jpain.2008.08.010>.
77. Craig, K.D., Whitfield, M.F., Grunau, R.V.E., Linton, J., and Hadjistavropoulos, H.D. (1993). Pain in the preterm neonate: behavioural and physiological indices. *Pain* *52*, 287–299. [https://doi.org/10.1016/0304-3959\(93\)90162-I](https://doi.org/10.1016/0304-3959(93)90162-I).
78. Riddell, R.R., Stevens, B.J., Cohen, L.L., Flora, D.B., and Greenberg, S. (2007). Predicting maternal and behavioral measures of infant pain: the relative contribution of maternal factors. *Pain* *133*, 138–149. <https://doi.org/10.1016/j.pain.2007.03.020>.
79. Koenig, T., Kottlow, M., Stein, M., and Melie-García, L. (2011). Ragu: a free tool for the analysis of EEG and MEG event-related scalp field data using global randomization statistics. *Comput. Intell. Neurosci.* *2011*, 938925. <https://doi.org/10.1155/2011/938925>.
80. Khanna, A., Pascual-Leone, A., Michel, C.M., and Farzan, F. (2015). Microstates in resting-state EEG: current status and future directions. *Neurosci. Biobehav. Rev.* *49*, 105–113. <https://doi.org/10.1016/j.neurobiorev.2014.12.010>.
81. Custo, A., Van De Ville, D., Wells, W.M., Tomescu, M.I., Brunet, D., and Michel, C.M. (2017). Electroencephalographic resting-state networks: source localization of microstates. *Brain Connect.* *7*, 671–682. <https://doi.org/10.1089/brain.2016.0476>.
82. Murray, M.M., Brunet, D., and Michel, C.M. (2008). Topographic ERP analyses: a step-by-step tutorial review. *Brain Topogr.* *20*, 249–264. <https://doi.org/10.1007/s10548-008-0054-5>.
83. Guthrie, D., and Buchwald, J.S. (1991). Significance testing of difference potentials. *Psychophysiology* *28*, 240–244. <https://doi.org/10.1111/j.1469-8986.1991.tb00417.x>.
84. Theiler, J., Eubank, S., Longtin, A., Galdrikian, B., and Doyne Farmer, J. (1992). Testing for nonlinearity in time series: the method of surrogate data. *Phys. D: Nonlinear Phenom.* *58*, 77–94. [https://doi.org/10.1016/0167-2789\(92\)90102-S](https://doi.org/10.1016/0167-2789(92)90102-S).
85. Prichard, D., and Theiler, J. (1994). Generating surrogate data for time series with several simultaneously measured variables. *Phys. Rev. Lett.* *73*, 951–954. <https://doi.org/10.1103/PhysRevLett.73.951>.
86. Theiler, J., and Prichard, D. (1996). Constrained-realization Monte-Carlo method for hypothesis testing. *Phys. D: Nonlinear Phenom.* *94*, 221–235. [https://doi.org/10.1016/0167-2789\(96\)00050-4](https://doi.org/10.1016/0167-2789(96)00050-4).

STAR★METHODS

KEY RESOURCES TABLE

| REAGENT or RESOURCE | SOURCE | IDENTIFIER |
|-------------------------------|---|-----------------|
| Software and algorithms | | |
| MATLAB R2016b | http://www.mathworks.com/products/matlab/ | RRID:SCR_001622 |
| EEGLAB 13_5_4b | http://sccn.ucsd.edu/eeglab/index.html | RRID:SCR_007292 |
| LabChart v8 | https://www.adinstruments.com/support/downloads/windows/labchart | N/A |
| Ragu | http://www.thomaskoenig.ch/index.php/software/ragu | RRID:SCR_016851 |
| Curry 8 | https://compumedicsneuroscan.com/products/by-name/curry/ | RRID:SCR_009546 |
| Neonatal Facial Coding System | Grunau and Craig ⁷² | N/A |

RESOURCE AVAILABILITY

Lead contact

Further information and requests for resources should be directed to and will be fulfilled by the Lead Contact, Lorenzo Fabrizi (l.fabrizi@ucl.ac.uk).

Materials availability

This study did not generate new, unique reagents or materials.

Data and code availability

- Pre-processed data reported in this paper will be shared by the [lead contact](#) upon reasonable request.
- Code used to analyse the data reported in this paper will be shared by the [lead contact](#) upon reasonable request.
- Any additional information required to reanalyse the data reported in this paper is available from the [lead contact](#) upon reasonable request.

EXPERIMENTAL MODEL AND SUBJECT DETAILS

Twenty human infants (32–44 completed postmenstrual weeks, 9 female; [Table 1](#)) who required a clinical blood test and were exposed to two consecutive sampling attempts (with heel lancing) were included in this study. This was an opportunistic sample from a larger database of 283 infants who were recruited from the Maternity and Neonatal Units at University College London Hospitals (UCLH) over 12 years between December 2007 and November 2019. The twenty infants included in this study underwent a second heel lance following an unsuccessful first attempt to collect the necessary amount of blood for a clinically-required test and no heel lance was performed solely for the purposes of research. Repeated heel lancing is not common in our units, but is reported elsewhere to occur in 49% of test occasions because of inexperience in conducting the procedure, unsuccessfully reaching the superficial dermal blood vessels, reduced blood flow from the cut, sample haemolysis or an insufficient blood sample for the desired screening test.¹⁷

No infants in this cohort were diagnosed with periventricular leukomalacia (PVL), germinal matrix-intraventricular haemorrhage (GM-IVH) greater than grade 2, intrauterine growth restriction (IUGR), trisomy 21, or presented any clinical signs of hypoxic ischaemic encephalopathy (HIE). Ethical approval for this study was given by the NHS Health Research Authority (London – Surrey Borders) and conformed to the standards set by the Declaration of Helsinki. Informed written parental consent was obtained before each study.

METHOD DETAILS

Repeated noxious stimuli

The repeated noxious stimuli were consecutive clinically required heel lances. All heel lances were performed by a trained neonatal nurse using disposable lancets and standard hospital practice. Infants were soothed as and when required. Parents could hold and feed their baby at will. The heel was cleaned with sterile water using sterile gauze and the lancet placed against the heel for at least 30 seconds prior to the release of the blade. This was to obtain a period of recording prior to the stimulus free from other stimulation that could be used as baseline. The heel was squeezed for blood collection only 30 seconds after the release of the blade, again to ensure a post-stimulus period free from other stimuli. The second lance was performed on the same heel due to clinical reasons

(i.e., extensive bruising or damage from previous lances still visible on the other heel) 3–18 minutes (median of 7.5 minutes) after the first (Figure 1B). Infants remained in the same position (in skin-to-skin contact with one of their parents, held with clothing or in cot with individualized care) throughout the recording session except for one. Some infants transitioned from one sleep state to another between first and second lance, however there was not a predominant sleep state transition or significant difference in the overall distribution across sleep states for the whole sample (preterm: $p=0.975$, term: $p=1.000$) (Figure S4).

Data collection

Brain electrical activity at the scalp (electroencephalography, EEG), flexion withdrawal reflex of the lanced leg (surface electromyography, EMG), heart rate changes (electrocardiography, ECG) and facial expressions (video) time-locked to the clinically-required heel lances were recorded (Figure 1A). EEG recordings were successful for both lances in all subjects ($n=20$; 40 recordings). EMG, ECG and video recordings were successful in 24 ($n=12$), 38 ($n=19$) and 36 ($n=19$) recordings respectively.

EEG recording and preprocessing

The electroencephalogram (EEG) was recorded from a subset of 19 recording electrodes (disposable Ag/AgCl cup electrodes) from the international 10/20 electrode placement system.⁷³ Those included electrodes overlying primary visual (O1, O2), primary auditory (T7, T8), association (F7, F3, Fz, F4, F8, P7, P8, T9, TP10), and somatosensory (C3, Cz, C4, CP3, CPz, CP4) cortices (Figure 1A). This set of electrodes balanced electrode-scalp coverage with cortical site representation. The reference electrode was placed at FCz or Fz and the ground electrode at FC1 or FC2 (depending on the position of the infant). Electrode/skin contact impedances were maintained below 10 kOhms when possible, by gently rubbing the skin with a prepping gel (NuPrep, Weavever & Co.) and then applying the electrodes with a conductive paste (10/20 Weaver & Co.). The Neuroscan SynAmps2 EEG/EP (Compumedics, USA) recording system was used to record EEG activity from DC to 500 Hz. Signals were digitized with a sampling rate of 2 kHz and a resolution of 24-bit. All EEG data was examined by a trained neurophysiologist and no EEG abnormalities were observed.

EEG data was pre-processed using MATLAB (2016, MathWorks, Inc.) and EEGLAB.⁷⁴ Raw data were filtered with a second-order bidirectional Butterworth bandpass (1–25 Hz) and a notch (48–52 Hz) filter, and epoched between 0.6 s prior to 1.5 s following the noxious stimulus. Raw data were subsequently de-noised using independent component analysis (between 0–3 discrete independent components per trial were removed corresponding to ECG breakthrough or muscle, movement or equipment artifacts, median: 0). Artifactual independent components were selected manually using the spatial maps and frequency content of the components. Spherical interpolation was then used to estimate data from channels that were not recorded (including the reference channel) or could not be denoised (maximum of four channels per trial, range: 0–4, median: 0). Independent components that required discarding and channels that required interpolating were identified by the same experienced researcher. We then applied DC correction, down-sampled the data to 512 Hz and re-referenced to the common average. In the group analysis, electrode positions were considered as contralateral or ipsilateral to the stimulus side, not according to their physical positions on the scalp (right vs left). For example, recording contralateral to the stimulus were averaged independently of whether they were recorded from the left or right side of the scalp (e.g., recording at C3 and C4 following right and left heel stimulation respectively were averaged).

EMG recording and preprocessing

The electromyogram (EMG) of the lanced leg was recorded from two self-adhesive surface silver/silver-chloride electrodes (Cardinal Health, USA) positioned over the biceps femoris (same ground as that used for EEG recording). The EMG was recorded as a bipolar signal with the same Neuroscan SynAmps2 system used for EEG, amplified ($\times 10,000$), and sampled at 2 kHz with a 24-bit resolution.

EMG data was pre-processed using custom-written scripts in MATLAB (2016, MathWorks, Inc.). EMG data from 9 out of the 12 subjects was of a quality suitable for analysis. Raw data were filtered with a second-order bidirectional Butterworth bandpass (10–500 Hz) and a notch (48–52 Hz) filter, and epoched between 1 s prior to 3 s following the stimulus. The EMG signal was then converted to z-scores to account for differences in signal amplitude across subjects possibly due to differences in electrode location relative to the biceps femoris and/or contact. The mean and standard deviation for z-scoring were computed from the baseline segments (1 s period prior to the stimulus) for each subject. The z-scored signal was then rectified, and low-pass filtered at 25 Hz (fourth-order bidirectional Butterworth). Artifactual segments were then identified using the median absolute deviation method (Matlab function 'mad.m') within a 1 s sliding window (50% overlap) as data points exceeding three standard deviations from the median signal.⁷⁵ Corrupted segments shorter than 0.05 s were replaced by spline interpolation using 0.05 s worth of data on either side of the corrupted segment, while segments longer than 0.05 s were discarded.

ECG recording and preprocessing

A lead I electrocardiogram (ECG) was recorded from two self-adhesive surface silver/silver-chloride electrodes (Cardinal Health, USA) positioned over both shoulders (same ground as that used for EEG recording). The ECG was recorded as a bipolar signal with the same Neuroscan SynAmps2 system used for EEG and EMG and sampled at 2 kHz with a 24-bit resolution.

ECG data was pre-processed using MATLAB (2016, MathWorks, Inc.) and LabChart (version 8, ADInstruments). Raw data were filtered with a second-order bidirectional Butterworth bandpass (0.5 – 45 Hz) filter. Beat-to-beat intervals (R-R intervals) were then automatically detected using the heart rate variability (HRV) module in LabChart and manually confirmed. The resulting signal (heart rate in beats per minute, BPM) was epoched between 30 s prior to and 30 s following the stimulus and baseline corrected using the 30 s period prior to the stimulus.

Facial expression recording and preprocessing

Facial expression were recorded on video and synchronized with the EEG recording with a light emitting diode placed within the frame that was activated by the blade release of the lancet.³⁰

Videos were reviewed offline by a trained behavioural coder. Videos were epoched between 10 s prior to and 10 s following the stimulus and infant facial expression were scored second-by-second according to the 7-item version of the Neonatal Facial Coding System (NFCS) (brow bulge, eye squeeze, nasolabial furrow, open lips, vertical stretch mouth, horizontal stretch mouth, and taut tongue).^{72,76,77} The facial actions were scored as either present (1) or not present (0) resulting in a percentage total score at each second (where a score of 100% indicates that all 7 facial actions were observed). Where the view of infants facial actions were partially/fully obstructed, data were estimated with conservative judgements based on either the assumption of facial symmetry, cry and body movements, and behaviours either side of the missing period.^{76,78} Partial estimates of facial expression score was made in 5 out of the 36 recordings.

EEG microstate analysis

Microstate EEG analysis was performed using Ragu^{28,79} and custom-written MATLAB scripts. Microstates are scalp potential fields which maintain a semi-stable topography over transient periods of 60-120 ms in adults^{10,80} and 150-300 ms in neonates.^{12,38,39} Microstate activation and switching across time represent changes in brain network engagement and information transfer.⁸¹ In this study, we considered microstates as a continuous phenomenon and took a geometric approach similar to that described in Mishra et al.,³⁷ where each microstate forms the vector basis of a reduced subspace of the original channel space. With this approach individual time points can be labelled as multiple microstates and microstate transitions are gradual rather than discrete.

We first determined our microstate basis on the entire dataset (i.e., using responses from first and second lance (repetition) in term and preterm (age) infants). To do that, we calculated the average response for each lance repetition and age group (four groups: first lance-term; second lance-term; first lance-preterm; second lance-preterm). For each of the four group averages, we calculated the global field power (GFP, standard deviation of the cortical activity across all electrodes at every timepoint; this is a single value which represents the strength of the signal as captured by the full electrode array). Next, we used a topographic consistency test (TCT) to identify spatially consistent event-related activity maps following the heel lance (Figure S1A).²⁸ The TCT assesses the similarity of the topography of scalp potentials within groups. Data at timepoints that have a significantly consistent topography across subjects reflect event-related activation, whereas random fluctuations in cortical activity, unrelated to the stimulus or not specific to the group, are unlikely to be consistent across participants at a given latency.²⁸ Significantly consistent timepoints were determined with bootstrapping. A non-parametric null distribution was obtained by shuffling data across electrodes for each subject (altering the consistency at each channel across subjects) and recalculating the GFP of the average (5000 iterations). If the true GFP of the average, at a given latency, was larger than the 95th percentile (right-tailed, $p < 0.05$) of the non-parametric null distribution, the topography was considered consistent.

Data from the four groups which were topographically consistent across subjects were then pooled in the same channel space and clustered to define our microstate basis. Clustering was performed with the aim to identify distinct topographies representing different cortical source configurations (in both location and/or orientation) that account for most of the variance in the data (Figure S1B). Clustering was performed using a modified hierarchical algorithm to that provided in the Ragu toolbox²⁸:

1. As part of a cross-validation process, the full dataset was randomly split into a training set (50%) and a test set (50%).
2. In the training set each sample was initially considered as the centre of its own distinct cluster.
3. Pair-wise spatial correlation between cluster centres was calculated leading to a covariance matrix.
4. Pairs of clusters whose centres were maximally correlated were merged and a new cluster centre was calculated as the average of the two original cluster centres. These formed the current template maps.
5. The explained variance in the test set was calculated for the template maps.
6. Steps 3 to 6 were repeated until we were left with two clusters. This led to an explained variance versus number of clusters relationship for a single cross-validation iteration.
7. 50 cross-validation iterations were repeated.
8. The 50 explained variance versus number of cluster relationships were averaged and the percentage change in the average variance explained between neighbouring cluster sets was calculated.
9. The optimal number of microstates to use was selected as the size of the last cluster set before the average variance explained dropped by more than 2% with another aggregation step. This choice represents a parsimonious use of microstates that still explain a considerable fraction of signal energy (in this case $\geq 80\%$ of the GFP).⁸²
10. The final microstate basis was determined on the full dataset.

Once the microstate basis was defined, we calculated the projection of each microstate on all data points of each lance repetition-age group.³⁷ The time period examined commenced at 200 ms prior to the stimulus trigger (-200 – 1500 ms) due to a period of uncertainty as to the exact release of the lance.³⁰

Finally, to understand whether the proximity of a data point to a microstate was above chance (i.e., whether a given microstate was indeed engaged at that time), we compared the projection value of the data point on each microstate against a non-parametric null distribution (Figure S1C). This was obtained by calculating the projection of that data point on a random topographic basis which

consisted of the baseline topographies (-600 – -200 ms) of all trials (subjects × lance trials × age) in the dataset. In order to consider the microstate significantly engaged, the projection value had to be above the 95th percentile of this null distribution, and the duration of significant engagement had to continue for longer than 5% of the post-lance period.⁸³ The periods in which microstates were significantly engaged were called *microstate occurrences*. Distinct occurrences of the same microstate were considered to be separated if the period in between was longer than 197 ms (this was the median duration across all microstate occurrences after projecting each data point of the first and second lance group average signals from term and preterm neonates on all microstates). Microstate occurrences that were separated by a duration shorter than this value were considered to be part of the same event.

The resulting projection pattern of microstates was then smoothed to eliminate states that, whilst significantly engaged, were sub-dominant with respect to the extent of the GFP they explained. This was performed by firstly identifying temporal regions where multiple states entirely co-existed (i.e., both the start and end time points of the co-existing microstates were the same, or the start and end times of one microstate fell completely within those of others). For these temporal regions, one or more co-existing microstates were identified as sub-dominant and discarded only if the extent of GFP they explained was less than the other microstate for more than 50% of the overlap duration.

QUANTIFICATION AND STATISTICAL ANALYSIS

Cortical response quantification and statistical comparison across ages and stimulus repetition

We firstly set out to statistically test differences in multichannel EEG responses following the first lance between term and preterm infants and then between first and second lance in the two age groups separately.

EEG microstates

From each smoothed projection pattern of microstates, we firstly calculated the onset, duration and total power for each microstate occurrence. Onset was the first time-point in which the projection value exceeded the significance threshold, duration was the difference between onset-offset (where offset is the last time-point in which the projection value exceeded the significance threshold) and total power was the overall amount of variance explained by the microstate across the whole occurrence duration.

Global event-related field topography differences between term and preterm responses (to the first lance) and first and second lance responses (in the two age groups separately) were tested by comparing these metrics for each microstate occurrence common to the two groups being tested. This was accomplished by comparing the observed difference in these metrics against a non-parametric null distribution. This was the distribution of the differences in these metrics calculated from an array of 5000 surrogate pairs of group averages obtained by phase randomising and resampling the collected dataset (see '[surrogate data generation](#)' for further details). Metric differences outside the 95% confidence interval (CI) of this null distribution were considered statistically significant.

ERP

We additionally tested for differences between term and preterm responses (to the first lance) and first and second lance responses (in the two age groups separately) on single channel recordings at Cz. The group ERP waveform was first estimated by averaging individual recordings at Cz across subjects for each stimulus trial. Significant differences between groups were determined at each sample by comparing differences against a non-parametric null distribution. This was the distribution of the same difference between an array of 5000 surrogate pairs of group averages obtained by phase randomising and resampling the collected datasets (see '[surrogate data generation](#)' for further details). To account for multiple testing, only continuous periods of samples outside the 95% CI that lasted for longer than 5% of the post-lance period were considered statistically significant.⁸³

Behavioural, spinal reflex, and autonomic response to a noxious stimulus quantification and analysis

We next assessed whether a lance stimulus elicited significant changes in EMG, ECG and facial expression in preterm and term infants separately. This analysis was conducted by comparing the signal following the first lance stimulus against baseline. Due to the high variability in neonate EMG, ECG and facial expression responses to the noxious stimuli, the median summary statistic was analysed for these measures as a method of more robustly capturing the central tendency for each dataset.

EMG

The median signal across subjects/temporal window was determined for three 1-second-long segments post-stimulus and compared against a non-parametric null distribution obtained from baselinedata. This was the distribution of the median value across subjects/temporal window of 1-second-long baseline segments from 5000 phase-randomised versions of the collected dataset (see '[surrogate data generation](#)' for further details). Phase randomisation was performed on the bandpass filtered baseline EMG signal before signal rectification. Post-stimulus changes were considered statistically significant if the median response was outside the 95% CI of this null distribution.

ECG

The median signal across subjects/temporal window was determined for three 10-second-long segments post-stimulus and compared against a null distribution obtained from baselinedata. This was the distribution of the median value across subjects/temporal window of 10-second-long baseline segments from 5000 phase-randomised versions of the collected dataset (see '[surrogate data generation](#)' for further details). Phase randomisation was performed on the processed heart rate signal. Post-stimulus changes were considered statistically significant if the median response was outside the 95% CI of this null distribution.

Facial expression

The median signal across subjects/temporal window was determined for two 3-second-long and one 4-second-long segments post-stimulus and compared against a null distribution obtained from baselinedata. This was the distribution of the median value across subjects/temporal window of two 3-second-long and one 4-second-long baseline segments from 5000 datasets obtained by bootstrapping 78 lance video-recordings (68 of which were not part of this study and a total of 41 video-recordings were those of preterm neonates). Post-stimulus changes were considered statistically significant if the median response was outside the 95% CI of this null distribution.

Behavioural, spinal reflex, and autonomic response statistical comparison across stimulus repetition

We lastly assessed differences in EMG, ECG and facial expression responses following first and second lance in term and preterm infants separately.

EMG

Significant differences between first and second lance were determined for three 1-second-long segments post-stimulus with non-parametric testing. The log ratio between the median signal across subjects/temporal window for all 1-second-long segments following first and second lance (baseline and post-stimulus periods) were calculated and compared against a null distribution. This was the distribution of the same ratio between an array of 5000 pairs of surrogate groups obtained by phase randomising and resampling the collected dataset (see '[surrogate data generation](#)' for further details). Phase randomisation was performed on the bandpass filtered EMG signal before signal rectification. Differences in post-stimulus temporal windows were considered statistically significant if the observed log ratio of the median responses was outside the 95% CI of this null distribution.

ECG

Significant differences between first and second lance were determined for three 10-second-long segments post-stimulus with non-parametric testing. The log ratio between the median signal across subjects/temporal window for all 10-second-long segments following first and second lance (baseline and post-stimulus periods) were calculated and compared against a null distribution. This was the distribution of the same ratio between an array of 5000 pairs of surrogate groups obtained by phase randomising and resampling the collected dataset (see '[surrogate data generation](#)' for further details). Phase randomisation was performed directly on the processed heart rate signals. Differences in post-stimulus temporal windows were considered statistically significant if the observed log ratio of the median responses was outside the 95% CI of this null distribution.

Facial expression

Significant differences between first and second lance were determined for two 3-second-long segments and one 4-second-long segment post-stimulus with non-parametric testing. The log ratio between the median signal across subjects/temporal window for these three segments following first and second lance were calculated and compared against a null distribution. This was the distribution of the same ratio between an array of 5000 pairs of groups obtained by resampling 78 lance video-recordings (68 of which were not included in this study). Differences in post-stimulus temporal windows were considered statistically significant if the observed log ratio of the median responses was outside the 95% CI of this null distribution.

Surrogate data generation

Phase randomisation is a method that enables surrogate data to be generated for statistical hypothesis testing.⁸⁴ Surrogate data can be used to form a null distribution for significance testing of original data as they can be considered as random copies of non-linear time series that preserve physiological correlations through the preservation of the signals power spectrum.⁸⁵

Each recording time-locked to a stimulus can be considered the linear sum of a signal of interest (i.e., the response to a stimulus) and a stationary random noise component. Based on the assumption that the signal is the same in each recording while the noise changes, conducting another recording should result in the data being a linear sum of the same signal but with different random noise. Creating surrogate data therefore consists of generating new random noise to add to the signal estimated from the recorded data. Surrogate data generation begins by isolating the noise from the signal by removing the group average (i.e., the non-stationary model component) from each subject's recording. This is not necessary when generating surrogate baseline segments as the recorded baseline is assumed to just represent stationary random noise with no signal. Each noise time-series is then converted into the frequency domain and the phase at each frequency is rotated by an independent random value between 0 and 2π .⁸⁴ Applying an inverse Fourier transformation leads to a new time series which has the same spectral characteristics of the original noise, but a different temporal realisation.⁸⁶ Finally, adding back the estimated signal (i.e., the group average or 0 for baseline) results in a new surrogate dataset, which can be used to generate a sample of the null non-parametric distribution of interest.

When comparing parameters between first and second lance the signal subtracted from the data to isolate the noise is estimated for first and second lance separately. However, to prevent the introduction of systematic differences between surrogate data when establishing the non-parametric null distribution, the signal added back at the end of the surrogate data generation process is the grand average across both lances. The surrogate time-series are then pooled together, and two new groups are formed with resampling. Differences between these two groups are a sample of the null distribution of interest.